

# Mesophase-Mediated Crystallization of Poly(butylene-2,6-naphthalate): An Example of Ostwald's Rule of Stages

Dario Cavallo,<sup>\*,†</sup> Daniela Mileva,<sup>‡,∇</sup> Giuseppe Portale,<sup>§</sup> Li Zhang,<sup>||</sup> Luigi Balzano,<sup>⊥</sup> Giovanni C. Alfonso,<sup>||</sup> and René Androsch<sup>‡</sup>

<sup>†</sup>Department of Mechanical Engineering, Eindhoven University of Technology, P.O. Box 513, 5600 MB Eindhoven, The Netherlands

<sup>‡</sup>Center of Engineering Sciences, Martin-Luther-University Halle-Wittenberg, D-06099 Halle/Saale, Germany

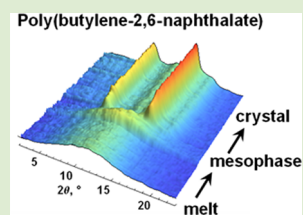
<sup>§</sup>DUBBLE CRG, European Synchrotron Radiation Facility, Netherlands Organization for Scientific Research (NWO), BP 220, F-38043, Grenoble Cedex, France

<sup>||</sup>Department of Chemistry and Industrial Chemistry, University of Genova, via Dodecaneso, 31-16146 Genova, Italy

<sup>⊥</sup>Material Science Center, DSM Ahead, P.O. Box 18, 6160MD, Geleen, The Netherlands

## Supporting Information

**ABSTRACT:** The investigation of poly(butylene-2,6-naphthalate) crystallization by means of chip-calorimetry and ultrafast wide-angle X-ray diffraction (WAXD) revealed the existence of two possible mechanisms. The formation of the stable triclinic  $\alpha$ -phase occurs directly from the undercooled melt at low cooling rates/high crystallization temperature. At higher cooling rates a two-stage route is observed: crystallization is preceded by the formation of a mesomorphic phase from the isotropic melt. The monotropic behavior of poly(butylene-2,6-naphthalate), becoming apparent only under severe cooling conditions, obeys the well-known Ostwald's rule of stages.



Poly(butylene-2,6-naphthalate) (PBN) is an aromatic polyester, considered an engineering plastic because of its excellent thermal and mechanical properties. As typically observed in semicrystalline polymers, these properties are related to the structure which develops during processing.

Two crystal modifications, the  $\alpha$ - and the  $\beta$ -forms, have been reported for PBN.<sup>1</sup> Both structures possess a triclinic unit cell<sup>1,2</sup> and form upon cooling from the melt;<sup>3–5</sup> the  $\beta$ -form prevails over the  $\alpha$ -form on crystallization at a low cooling rates/high temperatures.<sup>4,5</sup>

Recently, a mesophase has been identified in samples quenched from the melt.<sup>6</sup> This structure shows a degree of order intermediate between liquid and crystal and is characterized by a smectic periodicity of about 1.4 nm.

The formation of a mesomorphic phase in PBN does not represent an exception in the family of aromatic polyesters, since the aryl rings can typically act as mesogenic units.<sup>7–9</sup> Representative examples are the polyesters derived from bibenzoic acid and oxyalkylene glycols,<sup>10–14</sup> which can form liquid crystal (LC) phases even when copolymerized with a relatively high amount of 2,6-naphthalene dicarboxylate.<sup>13,14</sup>

In some of these systems, one or more mesophases appear as transient states on the route toward a more stable—usually crystalline—structure.<sup>14–19</sup> This behavior obeys the classical Ostwald's rule of stages,<sup>20</sup> which states that a phase transition proceeds via metastable states, whenever they exist, through stages of increasing stability. The importance of this empirical rule in the description of polymer crystallization has been reconsidered in the last two decades, on the basis of kinetics and thermodynamic arguments supporting its validity.<sup>21–24</sup> The role of metastable states in liquid–solid transitions is debated:

they can kinetically compete with the ultimately stable structure<sup>21–24</sup> or serve as precursors of crystallization, also for flexible chain polymers.<sup>25–27</sup>

A detailed study on the conditions for mesophase formation and on its role in the melt-crystallization process of PBN is still lacking, despite the relevance of this polymer as an engineering plastic. Indeed, the semirigid chain character coupled with high crystallizability may suggest a behavior in between that of conventional semicrystalline and mesogenic materials. The present work investigates PBN structuring in a wide range of undercooling, by means of fast scanning chip-calorimetry (FSC) and time-resolved X-ray scattering during fast cooling.

The apparent specific heat capacity of PBN cooled at different rates is plotted as a function of temperature in Figure 1. Three regions characterized by a qualitatively different crystallization behavior can be distinguished on variation of the cooling rate. Cooling at rates slower than 40 K s<sup>-1</sup> or faster than 400 K s<sup>-1</sup> reveals a single exothermic event. Instead, when cooling is performed at rates between 40 and 400 K s<sup>-1</sup>, two successive peaks are observed in the FSC curves.

On the basis of the information available in the literature, the exothermic event detected on slow cooling is assigned to  $\alpha$ -phase crystallization,<sup>3,5</sup> and the transition occurring on cooling faster than 400 K s<sup>-1</sup> is attributed to the formation of the mesophase.<sup>6</sup> Correspondingly, the observation of two exotherms in the intermediate range of cooling rates suggests a transition from an isotropic melt to the mesophase at high

Received: July 9, 2012

Accepted: July 31, 2012

Published: August 2, 2012

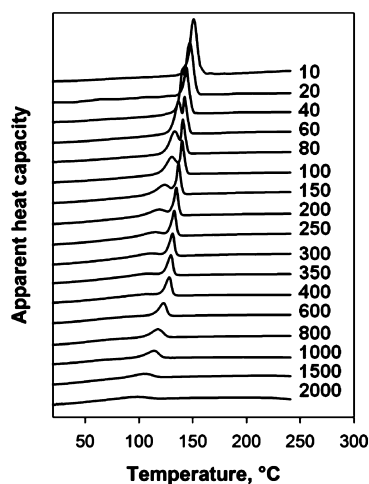


**Figure 1.** Apparent heat capacity as a function of temperature acquired on cooling from the PBN melt at the indicated rates (in  $\text{K s}^{-1}$ ).

temperature, followed by further crystallization from the mesomorphic state at lower temperatures. Such a behavior is typical of monotropic liquid-crystalline systems, in which case, however, it can be appreciated at standard differential scanning calorimetry (DSC) cooling rates.<sup>10,12,15–19,28–32</sup>

In agreement with this interpretation we notice that the high-temperature peak, detected on cooling faster than  $40 \text{ K s}^{-1}$  and related to mesophase formation, is rather sharp and shows only a minor dependence of the transition temperature on the applied cooling rate; in particular if compared with the crystallization peak at lower temperature. Moreover, while the low-temperature transition disappears on cooling faster than about  $400 \text{ K s}^{-1}$ , mesophase formation cannot be prevented even when cooling rates higher than  $1000 \text{ K s}^{-1}$  are imposed. This is analogous to the behavior observed in polymeric LC phases, whose formation experiences lower kinetic restrictions compared to crystallization, making it generally difficult to bypass all kinds of structuring and to obtain an isotropic glass.<sup>33</sup>

To support this interpretation, the structure formation of quenched thin polymer films was studied by time-resolved wide-angle X-ray diffraction (WAXD), according to a previously developed experimental method.<sup>34,35</sup> Figure 2 shows the structure obtained at room temperature, after completion of the solidification process, for samples submitted to the thermal histories reported in the Supporting Information, Figure S1. A pattern of an ice-quenched film recorded off-line is also included for the sake of comparison. Since in these ballistic cooling experiments the cooling rate is not constant,<sup>36</sup> the actual cooling rate at a temperature of  $170 \text{ }^\circ\text{C}$  is chosen as representative of the cooling process before structuring takes place.

In the range of cooling rates achievable with the used quenching device, that is, up to about  $150 \text{ K s}^{-1}$ , no change in the crystal structure obtained at room temperature is observed. The diffraction patterns indicate the presence of only the  $\alpha$ -phase<sup>1–5</sup> even at quenching conditions comparable to the FSC cooling experiments in which, as shown in Figure 1, two exothermic processes are detected. This supports the assignment of the second low-temperature transition to the mesophase-to-crystal transformation.

On the other hand, the ice-quenched sample presents the expected mesomorphic phase,<sup>6</sup> as noticed by the broad scattering in the WAXD region around a diffraction angle of

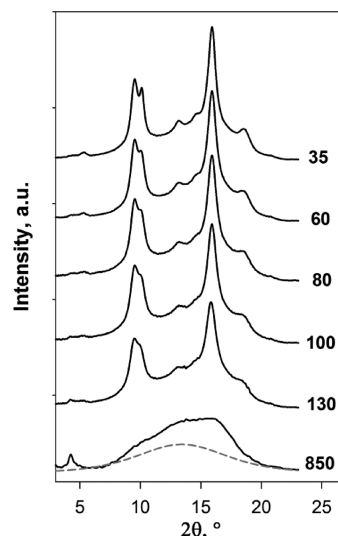


**Figure 2.** WAXD patterns of PBN films crystallized during ballistic cooling at the indicated rates (in  $\text{K s}^{-1}$ ). The dashed gray line represents the estimated amorphous scattering at room temperature.

$12^\circ$  and by detection of the smectic periodicity peak at low  $2\theta$ . It is worthwhile noting that the cooling rate applied for the preparation of this sample is higher than the one required to suppress the low-temperature mesophase-crystal transformation and is in the cooling-rate range where a single exothermic event is detected in the FSC curves of Figure 1.

A comparison with the X-ray pattern of an amorphous sample, estimated according to the procedure described in the Supporting Information (Figure S2), suggests that mesophase formation is not complete and a semimesomorphic sample has eventually been obtained, in agreement with literature results.<sup>6</sup> With respect to the isotropic liquid phase, excess scattering in the angular region between  $10$  and  $15^\circ$  of  $2\theta$  is evident and can be interpreted as an increased correlation in cross-chain direction.<sup>6</sup>

However, the examination of the room-temperature structure alone is not sufficient to demonstrate whether or not samples cooled in an intermediate range of cooling rates ( $60$ – $130 \text{ K s}^{-1}$ ) crystallized from a preordered mesophase. Ultimate evidence is gained from time-resolved WAXD experiments presented in Figure 3 for slowly and fast cooled PBN.

A dual crystallization behavior can be appreciated. For cooling rates lower than  $40 \text{ K s}^{-1}$ , when a single exothermic event is detected by chip-calorimetry, online WAXD data of Figure 3a confirm that crystallization of the  $\alpha$ -phase takes place directly from the isotropic melt. The data of Figure 3b, in contrast, demonstrate that on cooling at  $100 \text{ K s}^{-1}$  crystallization is preceded by mesophase formation, recognized by increased scattering at about  $12^\circ$  ( $2\theta$ ). The phenomenon is described in Figure S3 of the Supporting Information: the signal corresponding to the lower order structure rises well before the onset of crystallization, and this latter occurs directly at the expenses of the mesophase. Analogous results are obtained for cooling rates between  $80$  and  $130 \text{ K s}^{-1}$ .

Interestingly, no evidence of smectic periodicity at low diffraction angles can be observed for the mesophase. We deduce that mesophase formation proceeds by initial lateral correlation of molecular segments and, therefore, the mesomorphic state of PBN resembles a nematic phase in the early stages. However, a closer inspection of the room

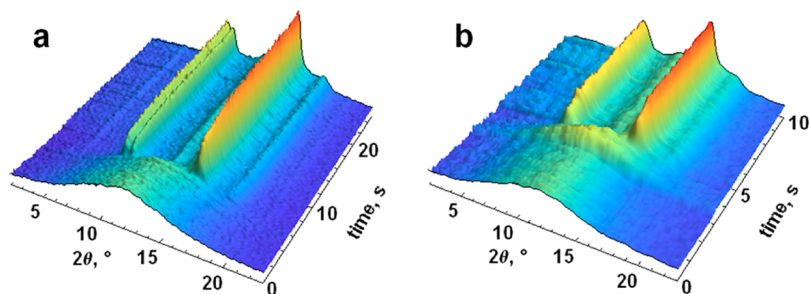


**Figure 3.** Time-resolved WAXD patterns during cooling PBN samples at approximately (a) 35 and (b) 100 K s<sup>-1</sup>.

temperature patterns of Figure 2 reveals that a faint trace of the diagnostic smectic peak is present for quenching rates between 60 and 130 K s<sup>-1</sup>.

On the basis of this argument we can speculate that, upon fast cooling,  $\alpha$ -phase crystallization is preceded by the formation of a nematic phase. The remaining amorphous material can undergo an isotropic–smectic transition followed by vitrification at the glass transition of this mesophase, suggested to be around 65 °C.<sup>6</sup> Indeed, a system constituted by crystals and smectic glass can be found when crystallization occurs from a mesophase.<sup>14,19</sup>

The above-described experimental observation, namely, crystal formation from the isotropic melt and from a metastable mesophase, are in agreement with results obtained by Keller and Cheng<sup>22–24</sup> for several polymer systems, including monotropic liquid-crystalline polymers.<sup>29,30,32</sup> A simple explanation can be given with the aid of Figure S4 of the Supporting Information. The rate of formation of stable and metastable phases below their respective equilibrium melting temperature is assumed to be controlled by an energy barrier for the nucleation process (either primary or secondary). Considering a lower equilibrium melting temperature and mean surface free energy for the metastable phase, it has been demonstrated<sup>21,22</sup> that the most probable situation will be a crossover of the rates of formation of the two structures, with mesophase kinetics becoming faster than that of crystalline phase below a given temperature  $T^*$  (see Figure S4 in the Supporting Information).

Three different situations can be envisaged, with respect to structure formation as a function of temperature.<sup>21–24</sup> In the temperature region between the equilibrium melting points of the stable and metastable phase ( $T_{m,stable}^{\circ}$  and  $T_{m,meta}^{\circ}$ , respectively), the isotropic melt transforms directly into the structure of ultimate stability, that is, the  $\alpha$ -phase in our case. For temperatures below  $T^*$ , the rate of formation of the mesophase is higher than that of crystallization. In this case a two-step process is observed: a first transition from the melt to the mesophase, followed by its transformation into the stable crystalline phase. The two phases have comparable transition rates in the temperature window  $T_{m,meta}^{\circ} - T^*$ , leading to a competition for the transformation of the isotropic melt. All of these three regimes have been actually observed experimentally in mesogenic polymers.<sup>19,30,32</sup>

Due to the high crystallization rate of PBN, rapid cooling conditions have to be applied to bypass melt-crystallization and to enter the region of faster mesophase formation (see Figures 1 and 3). Since we demonstrated that such conditions are now achievable, the interesting opportunity of studying crystal formation both from the amorphous and the mesomorphic state emerges.

Figure 4 shows examples of the signal detected by chip-calorimetry during the isothermal structuring of PBN at

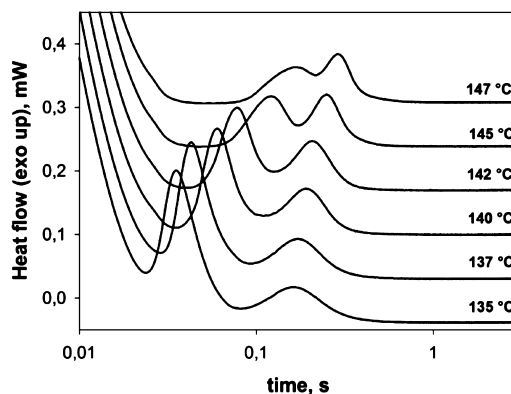


**Figure 4.** Heat flow as a function of time during isothermal crystallization of PBN at the indicated temperatures. An arbitrary vertical shift is applied to the curves for clarity.

different temperatures. Two separate exothermic peaks can be distinguished. In analogy with monotropic liquid-crystalline polymers,<sup>19,28,29</sup> we can identify the first process as being related to mesophase formation from the isotropic melt, while the second peak is interpreted as crystallization of the mesomorphic structure.

In contrast, when crystallization experiments are performed at low undercooling, the direct formation of the crystalline  $\alpha$ -phase from the melt results in a single exothermic peak, as shown in the DSC experiments reported in the Supporting Information, Figure S5.

In agreement with previous interpretation of the non-isothermal calorimetric and WAXD data, the time required for mesophase development shows a more pronounced decrease with temperature compared to crystal formation. In other words, the kinetics of mesophase formation has a stronger dependence on structuring temperature than crystallization kinetics. The two peaks tend to merge at higher temperatures, when the formation rates of the two polymorphs eventually become comparable.

The rates of the three transitions, that is, melt–crystal, melt–mesophase, and mesophase–crystal, are compared in Figure 5 for a large range of undercooling. Values are obtained by considering the reciprocal of the respective exothermic peak time at the chosen temperature.

The formation of mesophase prior to  $\alpha$  crystals is detected by Flash-DSC1 between 157 and 130 °C. Obviously, its development is expected also for lower temperatures, but it could not be observed experimentally due to the superposition

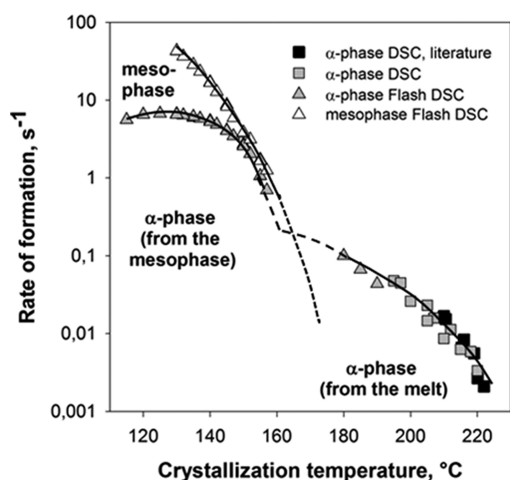


**Figure 5.** Rate of mesophase and crystal formation as a function of temperature. Lines are drawn to guide the eyes.  $\alpha$ -Phase crystallization kinetic data from the literature are added for comparison.<sup>37,38</sup>

with the initial instrumental thermal transient or because it occurred already during the cooling process.

At low undercooling, direct melt crystallization kinetics of the  $\alpha$ -phase could be probed reliably with DSC down to about 195 °C. Few more points at lower crystallization temperatures were obtained with chip-calorimetry, by measuring the increase of the melting enthalpy after different holding times at the transformation temperature. This strategy was not applicable for temperatures lower than 180 °C, because complex melting behavior involving multiple endotherms appeared, possibly indicative of the competitive growth of the two phases.

The rate of mesophase formation undergoes a much steeper increase with decreasing temperature than that of the  $\alpha$ -phase. Considering the trend of the kinetic data, the position of the crossover between crystal and mesophase formation rates can be expected around 165–170 °C. Moreover, also on the basis of the temperature of first detection of direct melt crystallization of the  $\alpha$ -phase, the isotropization temperature of the mesophase  $T_{m,meta}^{\circ}$ , that is, the temperature at which its rate of formation approaches zero, can be estimated in the vicinity of 180 °C. This value is about 100 °C lower than the equilibrium melting point of the triclinic  $\alpha$ -phase.<sup>4</sup>

By comparing the rate of  $\alpha$ -phase crystallization above and below 160 °C, the effect of the pre-existing mesophase on the phase transition kinetics can be immediately appreciated. Crystallization from the mesomorphic phase proceeds faster than from the melt and presents a maximum around 130 °C.

A similar acceleration of transformation kinetics when crystallization is preceded by liquid-crystal formation was reported by Cheng and Keller, both for smectogenic<sup>29</sup> and nematogenic<sup>30,32</sup> polymers. Jung et al. studied a poly(ester-imide) exhibiting both nematic and smectic phases formation followed by crystallization.<sup>31</sup> The kinetics of development of the ultimately stable crystalline structure decreases as a function of the degree of order of the precursor phase, that is, smectic–crystal > nematic–crystal > melt–crystal. The origin of the observed increase in the crystallization kinetics lays in a decrease of the energetic barrier for crystal nucleation<sup>31</sup> and/or growth,<sup>32</sup> due to the molecular orientational order introduced by the presence of the mesophase.

To summarize, in this letter a dual crystallization mechanism for poly(butylene-2,6-naphthalate) is revealed. At low cooling

rates/low undercoolings, crystallization of the triclinic  $\alpha$ -phase occurs directly from the melt. On increasing the cooling rate, the formation of the stable crystalline phase follows the appearance of a transient mesophase, as revealed by both chip-calorimetry and time-resolved WAXD during quenching. Above a critical cooling rate, crystallization can be kinetically prevented, and a semimesomorphic sample is obtained. The formation of the  $\alpha$ -phase following the two-stage route, that is, via the mesomorphic phase, presents a faster kinetics compared to the crystallization from the isotropic melt.

As demonstrated in this work, novel experimental methods which enable us to reach previously unattained conditions provide a tool to study mesophase-mediated crystallization in semicrystalline polymers.

## EXPERIMENTAL METHODS

Poly(butylene-2,6-naphthalate), free of additives and with an intrinsic viscosity of 1.05 dL/g, was kindly supplied by Teijin Shoji Europe GmbH.

Calorimetric data during fast cooling and isothermal crystallization at low temperatures were obtained with the Flash DSC1 from Mettler Toledo, coupled to a Huber intracooler TC45. PBN samples with a mass of about 400 ng were obtained by microtoming and cutting a compression molded film. The polymer was heated to 280 °C, annealed at this temperature for a period of 0.1 s, and subsequently cooled at different rates to –30 °C. Isothermal crystallization experiments included cooling the isotropic melt to predefined temperatures at a rate of 2000 K s<sup>-1</sup> and recording the exothermic heat flow for 5 s. More details about the device, sample preparation, and experimental procedure are reported in the literature.<sup>39</sup>

Time-resolved WAXD experiments were performed at the beamline BM26-DUBBLE of ESRF,<sup>40</sup> using an X-ray wavelength of 0.1033 nm. Polymer films with a thickness of about 250  $\mu$ m were wrapped in thin aluminum foils and annealed in the melt at 280 °C for 3 min. Subsequently, the films were quenched at different rates using a home-built cooling device. WAXD patterns were collected at frequency of 20 frames per s with a Pilatus 300K detector. Simultaneously, the sample temperature was acquired by means of a  $\mu$ -thermocouple inserted in the midplane of the polymer films. Further details on the experimental setup can be found elsewhere.<sup>34,35</sup>

## ASSOCIATED CONTENT

### Supporting Information

Thermal histories of quenched samples, experimental determination of amorphous scattering, evolution of crystal and mesophase intensities, scheme of stable and metastable phase formation rates, and DSC crystallization exotherms at low undercoolings. This material is available free of charge via the Internet at <http://pubs.acs.org>.

## AUTHOR INFORMATION

### Corresponding Author

\*E-mail: D.Cavallo1@tue.nl.

### Present Address

<sup>V</sup>Borealis Polyolefine GmbH, St. Peter-Str 25, 4021, Linz (Austria).

### Notes

The authors declare no competing financial interest.

## ACKNOWLEDGMENTS

The authors wish to thank N.I. Teijin Shoji Europe GmbH (Hamburg, Germany) for providing the investigated sample. The financial support by the German Research Foundation

(DFG) and the Netherland Organization for Scientific Research (NWO) is gratefully acknowledged.

## ■ REFERENCES

- (1) Watanabe, H. *Kobunshi Ronbunshu* **1976**, *33*, 229.
- (2) Koyano, H.; Yamamoto, Y.; Saito, Y.; Yamanobe, T.; Komoto, T. *Polymer* **1998**, *39*, 4385.
- (3) Chiba, T.; Asai, S.; Xu, W.; Sumita, M. *J. Polym. Sci., Part B: Polym. Phys.* **1999**, *37*, 561.
- (4) Ju, M.-Y.; Chang, F.-C. *Polymer* **2001**, *42*, 5037.
- (5) Ju, M.-Y.; Huang, J.-M.; Chang, F.-C. *Polymer* **2002**, *43*, 2065.
- (6) Konishi, T.; Nishida, K.; Matsuba, G.; Kanaya, T. *Macromolecules* **2008**, *41*, 3157.
- (7) Jackson, W. J. *Br. Polym. J.* **1980**, *12*, 154.
- (8) Economy, J. *J. Macromol. Sci., Part A: Chem.* **1984**, *21*, 1705.
- (9) Jin, J.-I.; Kang, C.-S. *Prog. Polym. Sci.* **1997**, *22*, 937.
- (10) Watanabe, J.; Hayashi, M. *Macromolecules* **1988**, *21*, 278.
- (11) Watanabe, J.; Hayashi, M. *Macromolecules* **1989**, *22*, 4083.
- (12) Bello, A.; Pereña, J. M.; Pérez, E.; Benavente, R. *Macromol. Symp.* **1994**, *84*, 297.
- (13) Chen, D.; Zachmann, H. G. *Polymer* **1991**, *32*, 1612.
- (14) Tokita, M.; Osada, K.; Watanabe, J. *Polym. J.* **1998**, *30*, 589.
- (15) Pérez-Manzano, J.; Fernández-Blázquez, J. P.; Bello, A.; Pérez, E. *Polym. Bull.* **2006**, *56*, 571.
- (16) Martínez-Gómez, A.; Pérez, E.; Bello, A. *Polymer* **2006**, *47*, 2080.
- (17) Hu, Y. S.; Hiltner, A.; Baer, E. *Polymer* **2006**, *47*, 2423.
- (18) Fernández-Blázquez, J. P.; Pérez-Manzano, J.; Bello, A.; Pérez, E. *Macromolecules* **2007**, *40*, 1775.
- (19) Heck, B.; Perez, E.; Strobl, G. *Macromolecules* **2010**, *43*, 4172.
- (20) Ostwald, W. *Z. Phys. Chem.* **1897**, *22*, 289.
- (21) Cheng, S. Z. D. *Phase transitions in polymers: the role of metastable states*; Elsevier: Amsterdam, 2008.
- (22) Keller, A.; Hikosaka, M.; Rastogi, S.; Toda, A.; Barham, P. J.; Goldbeck-Wood, G. *J. Mater. Sci.* **1994**, *29*, 2579.
- (23) Keller, A.; Cheng, S. Z. D. *Polymer* **1998**, *39*, 4461.
- (24) Cheng, S. Z. D.; Zhu, L.; Y. Li, C.; Honigfort, P. S.; Keller, A. *Thermochim. Acta* **1999**, *332*, 105.
- (25) Strobl, G. *Eur. Phys. J. E* **2000**, *3*, 165.
- (26) Strobl, G. *Prog. Polym. Sci.* **2006**, *31*, 398.
- (27) Strobl, G. *Rev. Mod. Phys.* **2009**, *81*, 1287.
- (28) Pardey, R.; Zhang, A.; Gabori, P. A.; Harris, F. W.; Cheng, S. Z. D.; Adduci, J.; Facinelli, J. V.; Lenz, R. W. *Macromolecules* **1992**, *25*, 5060.
- (29) Pardey, R.; Wu, S. S.; Chen, J.; Harris, F. W.; Cheng, S. Z. D.; Keller, A.; Adduci, J.; Facinelli, J. V.; Lenz, R. W. *Macromolecules* **1994**, *27*, 5794.
- (30) Heberer, D.; Keller, A.; Percec, V. *J. Polym. Sci., Part B: Polym. Phys.* **1995**, *33*, 1877.
- (31) Kim, S. O.; Koo, C. M.; Chung, I. J.; Jung, H.-T. *Macromolecules* **2001**, *34*, 8961.
- (32) Jing, A. J.; Taikum, O.; Li, C. Y.; Harris, F. W.; Cheng, S. Z. D. *Polymer* **2002**, *43*, 3431.
- (33) Tokita, M.; Funaoka, S.; Watanabe, J. *Macromolecules* **2004**, *37*, 9916.
- (34) Cavallo, D.; Portale, G.; Balzano, L.; Azzurri, F.; Bras, W.; Peters, G. W.; Alfonso, G. C. *Macromolecules* **2010**, *43*, 10208.
- (35) Cavallo, D.; Gardella, L.; Alfonso, G.; Portale, G.; Balzano, L.; Androsch, R. *Colloid Polym. Sci.* **2011**, *289*, 1073.
- (36) Cavallo, D.; Azzurri, F.; Floris, R.; Alfonso, G. C.; Balzano, L.; Peters, G. W. *Macromolecules* **2010**, *43*, 2890.
- (37) Lee, S. C.; Yoon, K. H.; Kim, J. H. *Polym. J.* **1997**, *29*, 1.
- (38) Achilias, D. S.; Papageorgiou, G. Z.; Karayannidis, G. P. *Macromol. Chem. Phys.* **2005**, *206*, 1511.
- (39) Kolesov, I.; Mileva, D.; Androsch, R.; Schick, C. *Polymer* **2011**, *52*, 5156.
- (40) Bras, W.; Dolbnya, I. P.; Detollenaere, D.; van Tol, R.; Malfois, M.; Greaves, G. N.; Ryan, A. J.; Heeley, E. *J. Appl. Crystallogr.* **2003**, *36*, 791.